Spectrochimica Acta Part A 83 (2011) 242–249

Contents lists available at SciVerse ScienceDirect

Spectrochimica Acta Part A: Molecular and Biomolecular Spectroscopy

journal homepage: www.elsevier.com/locate/saa

Experimental and theoretical study of two new pyrazoline derivatives based on dibenzofuran

He-ping Shi[a,c,*], Jian-xin Dai[a], Xiu-feng Zhang[a], Lei Xu[a], Long Wang[a], Li-wen Shi[a], Li Fang[a,b,**]

[a] School of Chemistry and Chemical Engineering, Shanxi University, Taiyuan 030006, PR China
[b] Engineering Research Center of Fine Chemicals, Ministry of Education, Taiyuan 030006, PR China
[c] Key Laboratory of Optoelectronic Materials Chemistry and Physics, Chinese Academy of Sciences, Fuzhou 350002, PR China

ARTICLE INFO

Article history:
Received 21 March 2011
Received in revised form 7 August 2011
Accepted 10 August 2011

Keywords:
Pyrazoline derivatives
Dibenzofuran
Fluorescence
TDDFT

ABSTRACT

Two novel pyrazoline derivatives, named 2,8-bis(1,3-diphenyl-pyrazoline-5-yl)dibenzofuran (**A**) and 2,8-bis(1-(4-bromophenyl)-3-phenyl-pyrazoline-5-yl)dibenzofuran (**B**), were synthesized and characterized by elemental analysis, NMR, MS and thermogravimetric analysis. The absorption and emission spectra of them were determined by experimental methods in different polar solvents and were computed using the density functional theory (DFT) and the time-dependent density functional theory (TDDFT) at the same time. The calculated absorption and emission wavelengths are in good agreement with the experimental data. The fluorescence quantum yields and fluorescence lifetimes of them in different polar solvents were studied by means of steady state and time resolved fluorescence. The calculated reorganization energy for hole and electron indicates that the two compounds are in favor of hole transport than electron transport. The results show the two compounds present high fluorescence quantum yields and excellent thermal stability. It makes them of great interest as novel fluorescent probes and optoelectronic materials.

1. Introduction

Since the first discovery of organic light-emitting diodes (OLEDs) by Tang and Van Slyke, light-emitting materials have attracted significant attention because of their potential applications in flat panel displays [1,2]. The most actively pursued areas of research are the improvement of efficiency and stability of the device and the tuning of color using different emitting materials. The continuing efforts include ingenious device fabrication and synthesis of materials with improved properties. Therefore, the design of novel light-emitting molecules has been a hot issue.

At present, the development of blue-emitting molecules with high efficiency and good color purity draws much attention, and there have been a great number of studies for new blue light-emitting materials that achieve higher efficiencies and have improved characteristics [3–6].

Pyrazoline derivatives are important five-membered, nitrogen-containing heterocyclic compounds and they have N atoms which attain conjugation by donating electron. They are attracting increasing interest of many researchers, not only in medicinal chemistry because of their bioactivity such as antimicrobial [7,8], antiamoebic [9,10], antinociceptive [11], anticancer [12], antidepressant [13] and antiinflammatory [14,15], but also in conjugated fluorescent dyes. They have high hole-transport efficiency, excellent blue emission and high quantum yields [16–18], which have been widely used as fluorescent brightening agents for textiles, fabrics, plastics and papers, fluorescence chemosensors, hole-transport materials in electrophotography, OLEDs and as a hole-conveying medium in photoconductive materials [19–28].

Many pyrazoline derivatives have been reported as hole-transport materials in organic electroluminescent devices (OLEDs). Jin et al. synthesized several pyrazoline derivatives with different electron withdrawing and pushing groups. The results indicated that the pyrazoline derivatives with both electron withdrawing and pushing substitutional groups were the optimistic candidate for electroluminescent emitter due to higher transfer efficiency from electric energy to light energy as well as larger luminance [29]. Wang et al. synthesized a pyrazoline derivative with the presence of anthryl substituent at position of the pyrazoline ring. It is concluded that photo-induced intramolecular energy transfer from the anthryl to pyrazoline moiety exists simultaneously with the charge transfer from N (1) to C (3) in the pyrazoline moiety in the excited state and both compete with each other [30]. Bai et al. synthesized several novel fluorescence dyes in which carbazole moiety was linked to pyrazoline molecule [31]. Recently, a series of new pyrazoline derivatives have been synthesized as efficient emitting materials in organic EL devices and their photophysical properties have been investigated in detail [32,33].

In our previous work, a series of compounds containing a heterocycle as the core have been synthesized and investigated via

* Corresponding author. Tel.: +86 351 7018094; fax: +86 351 7011688.
** Corresponding author.
E-mail address: hepingshi@sxu.edu.cn (H.-p. Shi).

1386-1425/$ – see front matter © 2011 Elsevier B.V. All rights reserved.
doi:10.1016/j.saa.2011.08.026

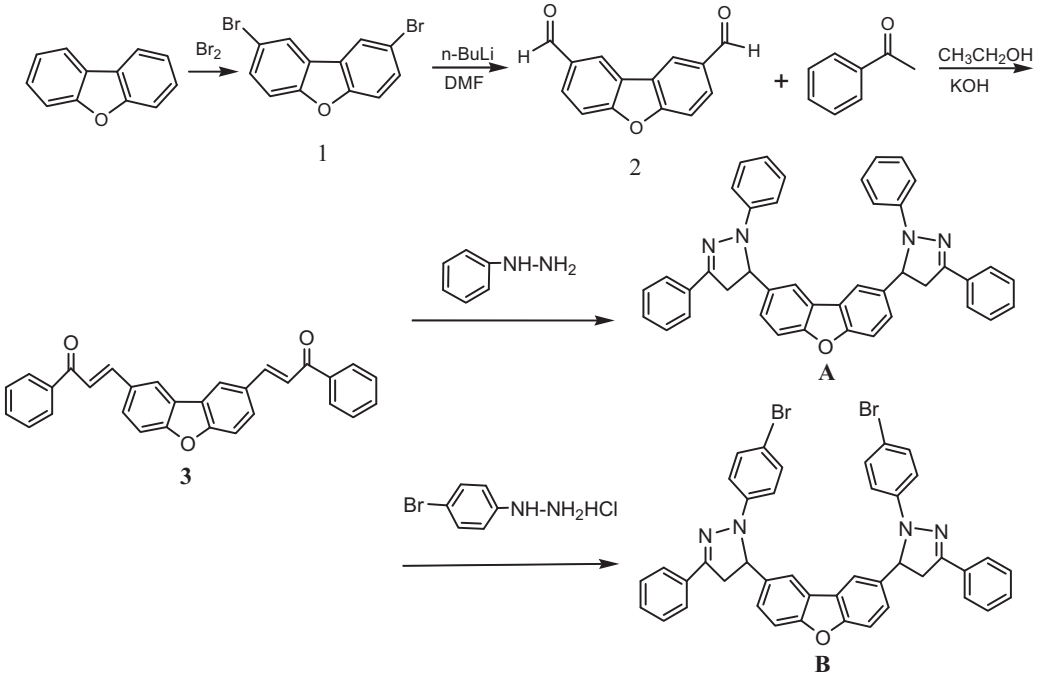

Scheme 1. The synthetic route of the compound A and B.

experimental and theoretical methods [34,35]. According to our research, we conclude the incorporation of electron-donors and electron-acceptors into one molecule should be highly desirable to improve optical properties.

In this paper, in view of the excellent optical properties of pyrazoline derivatives and our interest in the synthesizing analogous compounds involving fascinating diverse heterocycles, we designed and synthesized two novel pyrazoline derivatives containing two pyrazoline rings as side chains (electron-donors) and a dibenzofuran ring as the core (electron-acceptor). The synthetic route of the investigated compounds, named 2,8-bis(1,3-diphenyl-pyrazoline-5-yl)dibenzofuran (A) and 2,8-bis(1-(4-bromophenyl)-3-phenyl-pyrazoline-5-yl)dibenzofuran (B), is shown in Scheme 1. Their structures were characterized by elemental analysis, IR, NMR and MS. Furthermore, their charge injection and transport properties and spectral properties were studied by experimental and theoretical methods. In combination of pyrazoline rings with dibenzofuran molecule, we anticipate the formation of novel optical materials with excellent thermal stability and eminent photophysical properties. The results will increase the knowledge to design and synthesize novel pyrazoline derivatives with excellent optical properties.

2. Experimental

2.1. Materials and methods

2.1.1. Reagents and apparatus

Dibenzofuran and *n*-butyl lithium were purchased from Alfa Aesar and used without further purifications, other reagents were purchased from Beijing Chemical plants. Hexane, ethanol, DMF and benzene etc. were purified according to standard methods. All the reactions were carried out under nitrogen atmosphere.

Melting points were determined on an X-5 melting point detector and uncorrected. All NMR spectra were measured on a Bruker DRX-300 spectrometer with $CDCl_3$ or DMSO-d_6 as solvent. Thermogravimetric analyses were performed with a TA TGA 2050 thermogravimetric analyzer under nitrogen atmosphere with a heating rate of 20 °C/min from room temperature to 600 °C. Elemental analyses were performed with an Elementar Analysensysteme (GmbH). Mass spectra were recorded with the LC–MS system consisted of a Waters 1525 pump and a Micromass ZQ4000 singlequadrupole mass spectrometer detector (Waters). UV–vis spectra were obtained on a shimadzu UV-2450 spectrophotometer. Fluorescence spectra were obtained on a Shimadzu RF-5301PC fluorothotometer. Fluorecence quantum yields were determined using the a standard actinometry method. Quinine sulfate was used in the actinometer with a known fluorescence quantum yield of 0.55 in 0.1 mol/L sulphuric acid, the sample was excited at 350 nm. The fluorescence decay curves were recorded with time-correlated single photon counting (TCSPC) technique using a commercially available Edinburgh Instruments.

2.1.2. Procedures

The syntheses of the two compounds were described in Section 2.2. All spectral experiments were carried out at room temperature. The concentration of compounds is 1.0×10^{-5} mol/L in spectral experiments. All emission spectra were corrected. Excitation and emission slits width were both set at 2.5 nm.

2.2. Synthesis and characterization

2.2.1. Synthesis of 2,8-dibromodibenzofuran (1)

A 250 ml round bottom flask containing 8.4 g (50 mmol) of dibenzofuran dissolved in 100 ml of glacial acetic acid was equipped with an addition funnel. Bromine 5.13 ml (100 mmol) in 30 ml of glacial acetic acid was added dropwise via the addition funnel to the dibenzofuran under constant stirring. This reaction mixture was stirred at room temperature for 4 h. It was then refluxed for 6 h, cooled. The solid was then collected by filtration and washed with three 100 ml portions of water. Recrystallization from 100 ml of acetic anhydride obtained 12.2 g (75%) pure 2,8-dibromodibenzofuran (**1**) as a white solid; m.p. 188–190 °C; ^{1}H

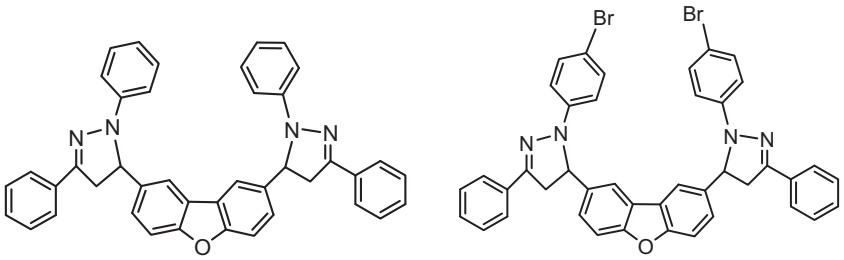

Fig. 1. The molecular structures as calculation models.

NMR ($CDCl_3$, 300 MHz): δ 7.17 (d, 2H), 7.58 (d, 2H), 8.15 (d, 2H) ppm.

2.2.2. Synthesis of 2,8-diformyldibenzofuran (2)

To a well-stirred suspension of 3 g (9.2 mmol) of 2,8-dibromodibenzofuran (**1**) in 45 ml of dry ether under a nitrogen atmosphere at −78 °C in a dry ice/acetone bath was added 8.1 ml (20.24 mmol) of a 2.5 M solution of *n*-butyl lithium in hexane. The resulting suspension was allowed to warm to room temperature and was stirred for 2 h. Then it was added 2.14 ml (27.6 mmol) of DMF under a nitrogen atmosphere at −78 °C in a dry ice/acetone bath. The mixture was allowed to gradually warm to room temperature for 8 h. After addition 10% aqueous hydrochloric acid solution, the precipitated solid was collected by filtration, washed with water, dried. The product was crystallized from dry ether and 1.6 g of white solid was obtained. The yield was 78%; m.p. 192–194 °C; IR (KBr) (cm^{-1}): 3426, ν_{C-H} (dibenzofuran); 2925, 2852, ν_{C-H} (–CHO); 1695, $\nu_{C=O}$ (–CHO); 1631, 1594, 1470, $\nu_{C=C}$ (dibenzofuran); 900–700, ν_{C-H} (dibenzofuran); ^{1}H NMR (300 MHz, $CDCl_3$): δ 7.67 (s, 2H), 8.05 (s, 2H), 8.69 (s, 2H), 10.09 (s, 2H) ppm.

2.2.3. Synthesis of chalcone based on dibenzofuran (3)

0.5 g (2.23 mmol) of 2,8-diformyldibenzofuran (**2**), 43 ml (4.46 mmol) of acetophenone and 30 ml of ethanol were added in 100 ml conical flask, and the solution was obtained by stirring at room temperature. Then 10% KOH aqueous solution (5 ml) was dropped in. The reaction was kept for 24 h at room temperature. The solid was obtained after filtration, and the product was recrystallized from anhydrous ethanol after washed by distilled water. The 0.66 g of light yellow powder was obtained. The yield was 69%; m.p. 248–250 °C; IR (KBr) (cm^{-1}): 1628 (–CO–); ^{1}H NMR (300 MHz, $CDCl_3$): δ 6.83 (2H), 8.37–7.47 (16H) ppm.

2.2.4. Synthesis of 2,8-bis(1,3-diphenyl-pyrazoline-5-yl) dibenzofuran (A)

A mixture of 0.506 g (1.18 mmol) **3** and phenylhydrazine 0.26 ml (2.6 mmol) in 15 ml of glacial acetic acid and 15 ml of ethanol was heated under reflux for 6 h. The solid product obtained on cooling was filtered, washed with ethanol and crystallized from ethanol. 0.438 g yellow solid powder was obtained. The yield was 80%; m.p. 176–178 °C; IR (KBr) (cm^{-1}): 3416, ν_{C-H} (dibenzofuran skeleton); 1598, $\nu_{C=N}$ (pyrazoline ring); 1489, 1345, ν_{C-H} (pyrazoline ring, $-CH_2-$, –CH–). ^{1}H NMR (300 MHz, DMSO-d_6): δ 3.21 (2H, the $-CH_2-$ of pyrazoline ring), 4.01 (2H, the $-CH_2-$ of pyrazoline ring), 5.61 (2H, the –CH= of pyrazoline ring), 6.71–8.31 (26H, phenyl, dibenzofuran-skeleton) ppm; ^{13}C NMR (300 MHz, DMSO-d_6): δ 53.4, 74.8, 114.3, 115.9, 117.9, 122.2, 128.7, 130.3, 131.4, 136.6, 143.5, 146.2, 147.6, 159.5 ppm; MS (*m*/*z*): 608.2687 (M^+); Anal. Calcd for $C_{42}H_{32}N_4O$: C, 82.87; H, 5.30; N, 9.20; Found: C, 82.69; H, 5.17; N, 9.06.

2.2.5. Synthesis of 2,8-bis(1-(4-bromophenyl)-3-phenyl-pyrazoline-5-yl)dibenzofuran (B)

A mixture of 1 g (2.33 mmol) **3** and 4-bromophenylhydrazine hydrochloride 1.15 g (5.13 mmol) in 30 ml of ethanol was heated under reflux for 6 h. The solid product obtained on cooling was filtered, washed with ethanol and crystallized from ethanol. 1.22 g light yellow solid powder was obtained. The yield was 84%; m.p. 238–240 °C; IR (KBr) (cm^{-1}): 3426, ν_{C-H} (dibenzofuran-skeleton); 1598, $\nu_{C=N}$ (pyrazoline ring); 1490, 1351, ν_{C-H} (pyrazoline ring, $-CH_2-$, –CH–). ^{1}H NMR (300 MHz, DMSO-d_6): δ 3.22 (2H, the $-CH_2-$ of pyrazoline ring), 4.02 (2H, the $-CH_2-$ of pyrazoline ring); 5.71 (2H, the –CH= of pyrazoline ring); 7.0–8.11 (25H, phenyl, dibenzofuran-skeleton) ppm; ^{13}C NMR (300 MHz, DMSO-d_6): δ 53.5, 74.5, 115.7, 119.3, 122.0, 129.0, 131.0, 134.3, 135.5, 136.3, 143.3, 145.3, 148.8, 159.4 ppm; MS (*m*/*z*): 766.0892 (M^+); Anal. Calcd for $C_{42}H_{30}Br_2N_4O$: C, 65.81; H, 3.94; N, 7.31; Found: C, 65.65; H, 3.82; N, 7.23.

The thermal stability of the two pyrazoline derivatives was measured using thermogravimetric analysis (TGA). The result reveals that two pyrazoline derivatives exhibit excellent thermal stability up to 250 °C and 280 °C, respectively.

2.3. Computational procedures

The ground-state geometries as well as their ionic structures of two pyrazoline derivatives were optimized at B3LYP level with 6-31G(d, p) basis set [36,37]. The vibration frequencies and the frontier molecular orbital characteristics were analyzed on the optimized structures at the same level. The ionization potential (IP), electron affinity (EA), reorganization energy, and HOMO–LUMO gap of them were calculated by DFT method based on the optimized geometry of the neutral and ionic molecules. The excited-state geometries of two pyrazoline derivatives were optimized at the configuration interaction with single excitation (CIS) level with 6-31G (d, p) basis set [38]. The absorption spectra and the emission spectra of the two pyrazoline derivatives were carried out using time-dependent density functional theory (TDDFT) method based on the optimized ground state structures and the lowest singlet excited-state structures, respectively. Solvent effects were also taken into account by using the polarized continuum model (PCM) [39,40]. All calculations were carried out with the Gaussian03 program package [41]. All the calculations were performed using the advanced computing facilities of supercomputing center of computer network information center of Chinese Academy of Sciences. The molecular structures as calculation models are shown in Fig. 1.

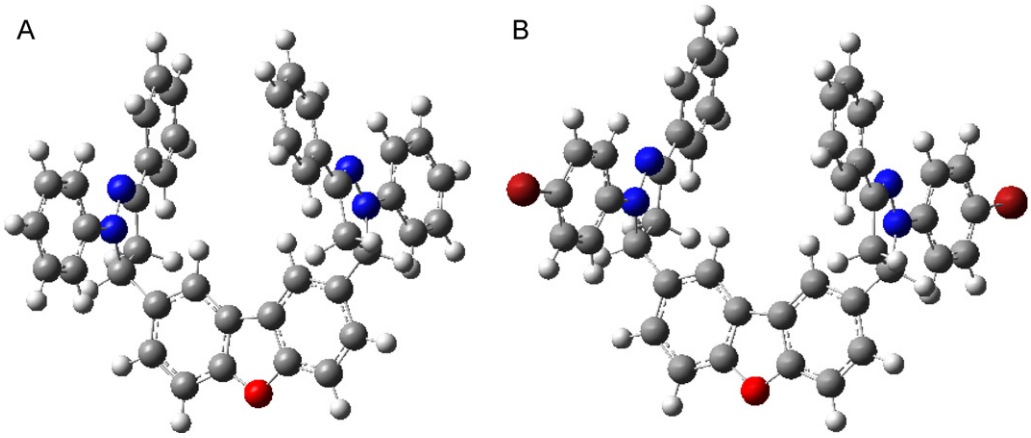

Fig. 2. The optimized geometry of the compound A and B in the ground state.

3. Results and discussions

3.1. Synthesis

In this paper, we described methods for the preparation of pyrazoline derivatives based on dibenzofuran. First, 2,8-dibromodibenzofuran (**1**) was synthesized via the reaction of dibenzofuran with bromine. Second, 2,8-diformyldibenzofuran (**2**) was obtained as the key intermediate for the whole procedure as shown in Scheme 1 via the reaction of 1 with *n*-butyl lithium and DMF. Third, chalcone based on dibenzofuran (**3**) was prepared by the reaction of **2** with acetophenone. Fourth, the two pyrazoline derivatives (**A** and **B**) were resulted by the reaction of **3** with phenylhydrazine and 4-bromophenylhydrazine hydrochloride, respectively. All of the novel compounds were characterized by elemental analysis, IR, NMR and MS, further details are given in Section 2.2.

3.2. Structures of pyrazoline derivatives

The optimized geometries of two pyrazoline derivatives in the ground state are shown in Fig. 2, and the optimized geometrical parameters for the two pyrazoline derivatives in the ground state are compiled in Table S1 (in SI). According to the data listed in Table S1, we can see the two pyrazoline derivatives possess similar molecular structures. Each derivative contains one planar moiety and two side chain moieties in its molecular structure, the planar moiety is dibenzofuran ring and two side chain moieties are pyrazoline rings. The dihedral angles C11–C13–C14–C15, C11–C13–N33–N16, C6–C23–C24–C25 and C6–C23–N34–N26 of the two moiety are 124.00°, −124.73°, −123.83° and 124.56° as well as 121.78°, −122.58°, −121.68° and 122.47° in compound A and B, respectively. It is indicated that the two pyrazoline derivatives possess the distorted geometrical structures.

3.3. Frontier molecular orbitals

The frontier molecular orbitals are the most important theory in determining the capability of electron or hole transport of molecules and the spectral properties [42].

The contour plots of HOMO and LUMO of the two pyrazoline derivatives are exhibited in Fig. 3. It can be seen from Fig. 3 that the election densities of HOMOs of the two pyrazoline derivatives are also localized on two pyrazoline side chains mainly. They are π-bonding orbitals. The election densities of LUMOs of the two pyrazoline derivatives are localized on the dibenzofuran core mainly. They are π^*-bonding orbitals. The electronic transition from the ground state to the excited state is mainly about an electron flowing from the pyrazoline side to the dibenzofuran core, which belongs to $\pi \rightarrow \pi^*$ transition. The energies of the HOMO, LUMO and energy gap are given in Table 1.

Table 1
HOMO and LUMO energies, and HOMO-LUMO energy gap of the compound A and B obtained from DFT/B3LYP/6-31G(d, p) calculation (eV).

	Methods	HOMO	LUMO	ΔE
Compound A	DFT-B3LYP/6-31G(d, p)	−4.871	−1.197	3.674
Compound B	DFT-B3LYP/6-31G(d, p)	−5.061	−1.388	3.674

3.4. Charge injection and transport properties

The charge injection and transport ability are important parameters for OLEDs. Normally, the energy barrier for injection holes and electrons are assessed by ionization potential (IP) and electronic affinity (EA). In general, the higher EA value of the electron transport layer (ETL), the easier the entrance of electrons from cathode to ETL, and the lower IP value of the hole-transport layer (HTL), the easier the entrance of holes from ITO to HTL. Therefore, we calculated their ionization potentials, electronic affinities. The calculated results are listed in Table 2. As shown in Table 2, the compound **A** has lower IP value, it is easier to transport hole than compound **B** and the compound **A** has higher EA value, it is easier to transport electron than compound **B**. The results are consistent with the indication from the energies analysis of their HOMOs and LUMOs.

A hopping model is often used to describe the charge mobility in organic materials, and the charge transport rate can be approximated by the Marcus electron-transfer theory with Eq. (1) [43].

$$k_{\text{hole/electron}} = \frac{4\pi^2}{h} \frac{1}{\sqrt{4\pi\lambda_{\text{hole/electron}} k_B T}} t^2 \exp\left(-\frac{\lambda_{\text{hole/electron}}}{4k_B T}\right) \quad (1)$$

where h is Planck's constant, $\lambda_{\text{hole/electron}}$ is the reorganization energy for hole or electron transfer between both molecules, k_B is Boltzmann's constants, T is the temperature and t is the

Table 2
Ionization potentials, electron affinities and reorganization energy of the compound A and B obtained from DFT/B3LYP/6-31G(d, p) calculation(eV).

Compound	IP_v	IP_a	λ_{Hol}	EA_v	EA_a	λ_{Ele}
Compound **A**	5.898	5.816	0.178	0.167	0.278	0.206
Compound **B**	6.023	5.9379	0.201	0.348	0.466	0.233

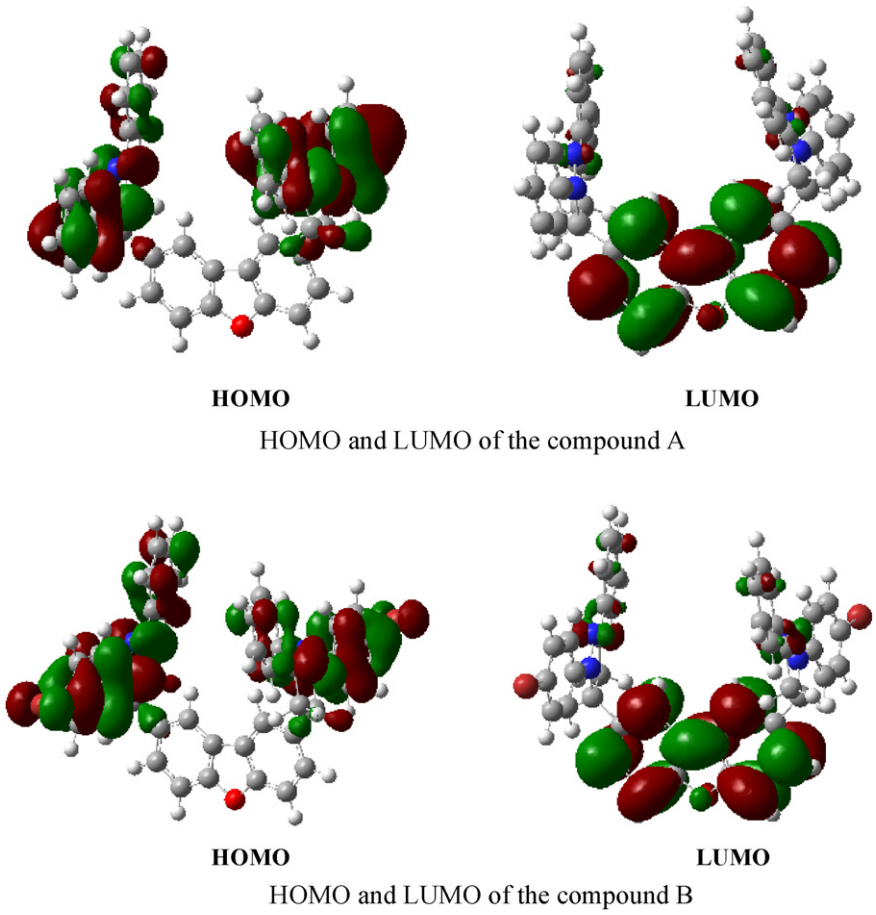

Fig. 3. The contour plots of HOMOs and LUMOs of the compound A and B in the ground state.

electronic transfer integral between the donor and acceptor molecules. Hence, the transport process is decided by two important Molecular factors: the intermolecular hole or electron transfer integral (t) which describes the strength of the electronic coupling between adjacent molecules and the reorganization energy (λ) which needs to be small for an efficient charge-transport [44].

The sum of two contributions, $\lambda_{+1} + \lambda_{+2}$ is the reorganization energy for hole transfer λ_{hole}, that are defined as

$$\lambda_{+1} = E_0(M^+) - E_0(M) \quad (2)$$

$$\lambda_{+2} = E_1(M) - E_1(M^+) \quad (3)$$

where $E_0(M^+)$ and $E_0(M)$ are the energies of the neutral molecule at the cation geometry and the optimal ground-state geometry, respectively. E_1(M) and $E_1(M^+)$ represent the energy of the charged state at the neutral geometry and optimal cation geometry, respectively.

Similarly, the sum of two contributions, $\lambda_{-1} + \lambda_{-2}$ is the reorganization energy for electron transfer $\lambda_{electron}$, that are defined as

$$\lambda_{-1} = E_0(M^-) - E_0(M) \quad (4)$$

$$\lambda^{-2} = E_1(M) - E_1(M^-) \quad (5)$$

where $E_0(M^-)$ and $E_0(M)$ is the energies of the neutral molecule at the anion geometry and the optimal ground-state geometry, respectively. $E_1(M)$ and $E_1(M^-)$ represent the energy of the charged state at the neutral geometry and optimal anion geometry, respectively.

According to the calculated model above, the calculated reorganization energy for hole and electron are listed in Table 2 where λ_{hole} exhibits lower value than corresponding $\lambda_{electron}$. It indicates that the two compounds are in favor of hole transport than electron transport, thus they are potential hole transport materials.

Table 3
UV–vis spectra and fluorescence spectra data of the compound A and B in different polar solvents.

Compounds	Solvents	UV wavelengths (λ, nm)	FL wavelengths (λ, nm)	Stokes shift (cm^{-1})
Compound A	Toluene	360	439	4999
	Ethylacetate	358	446	5511
	Chloroform	359	449	5584
	DMF	361	452	5577
	DMSO	360	455	5800
Compound B	Toluene	364	440	4745
	Ethylacetate	359	441	5179
	Chloroform	360	448	5457
	DMF	362	451	5452
	DMSO	365	454	5371

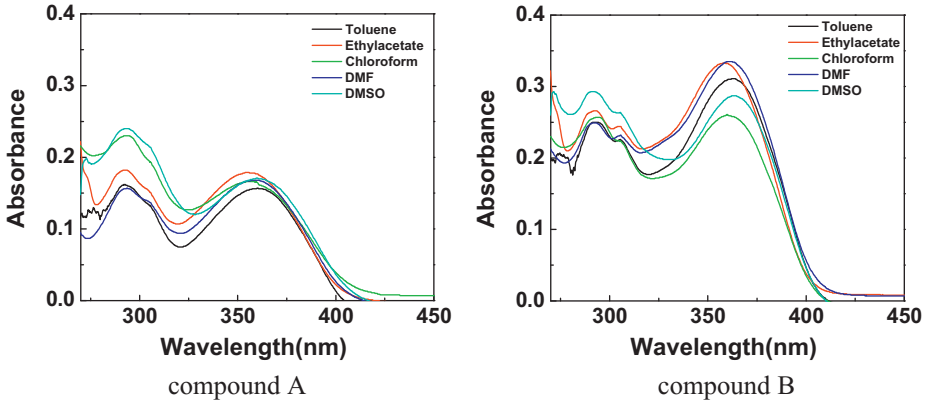

Fig. 4. Absorption spectra of the compound A and B in different polar solvents.

3.5. UV–vis spectra of the two pyrazoline derivatives

The UV–vis absorption spectra of the two pyrazoline derivatives have been studied in different polar solvents and the spectral data are collected in Table 3. The spectra are shown in Fig. 4. The two pyrazoline derivatives have similar absorption spectra. As indicated in the absorption spectra, each derivative exhibits two main bands at 270–320 and 320–400 nm due to $\pi \rightarrow \pi^*$ electronic transitions, which are almost the same in different polar solvents meaning the independence of UV absorption to the solvent polarity. The low-energy broad band at 320–400 nm is assigned to an intramolecular charge transfer (CT) band from the pyrazoline side rings of each derivative to the dibenzofuran ring of each compound in different polar solvents.

We computed singlet–singlet electronic transition in different polar solvents based on the optimized geometries of the ground state of the two compounds using time-dependent DFT method at the B3LYP/6-31G (d, p) level in order to gain a detailed insight into the nature of the UV–vis absorption of the two pyrazoline derivatives observed experimentally. The computed data of vertical electronic transitions of $S_0 \rightarrow S_1$, $S_0 \rightarrow S_2$, $S_0 \rightarrow S_3$, $S_0 \rightarrow S_4$ and $S_0 \rightarrow S_5$ are collected in Table S2 (in SI). The continuous absorption spectra were simulated with the help of SWIZARD software with the width at half-height of 2500 cm^{-1} on the basis of the calculated vertical excited energy and their corresponding oscillator strengths. The simulated absorption spectra of the two compounds are shown in Fig. S1(in SI). As seen in Fig. S1 and Table S2, the electronic transitions are of $\pi \rightarrow \pi^*$ type. The calculated $S_0 \rightarrow S_4$ excitation energy, oscillator strength of the two compounds in different polar solvents are 27,548–27,782 cm^{-1}, 1.1763–1.2413 and 27,326–27,743 cm^{-1}, 1.1025–1.2724, respectively. All the electronic transitions herein are strongly allowed. The calculated $S_0 \rightarrow S_1$ vertical excitation energy data of the two compounds are in good agreement with the experimental data.

3.6. Fluorescence spectra of the two pyrazoline derivatives

The steady-state fluorescence spectra of two compounds were measured in different polar solvents and shown in Fig. 5. Their spectral data are also collected in Table 3. The emission spectra of the two compounds consist of one broad band. This band can be assigned to the $S_1 \rightarrow S_0$ electronic transition. The spectra of the two compounds show a small shift in different polar solvents. As can be seen in Fig. 5 and Table 3, with the solvent changes from toluene to DMSO, the maximum emission wavelengths of the two compounds are redshifted from 439 to 455 nm and 440 to 454 nm, respectively. The Stoke's shifts for the two compounds are small in different polar solvents showing the relative rigidity of the two compounds.

In order to gain insight into the nature of the fluorescence emission observed for two compounds, the geometries of the first excited singlet state (S_1) were optimized for the two compounds. The optimized geometrical parameters for the two compounds in the first excited state are also compiled in Table S1. According to the data listed in Table S1, it can be see that the two compounds possess similar molecular structures in the first excited state and in the ground state, respectively. The dihedral angles C11–C13–C14–C15, C11–C13–N33–N16, C6–C23–C24–C25 and C6–C23–N34–N26 of the two moiety are 137.95°, −139.08°, −96.93° and 99.21°as well

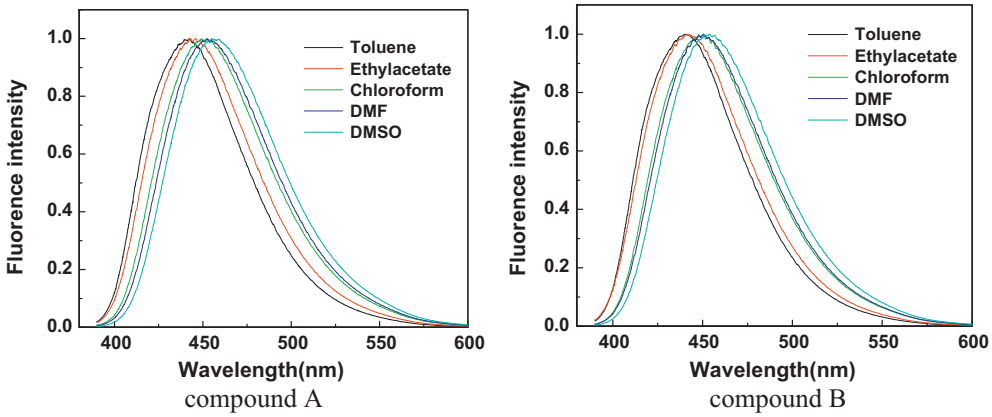

Fig. 5. The fluorescence spectra of the compound A and B in different polar solvents.

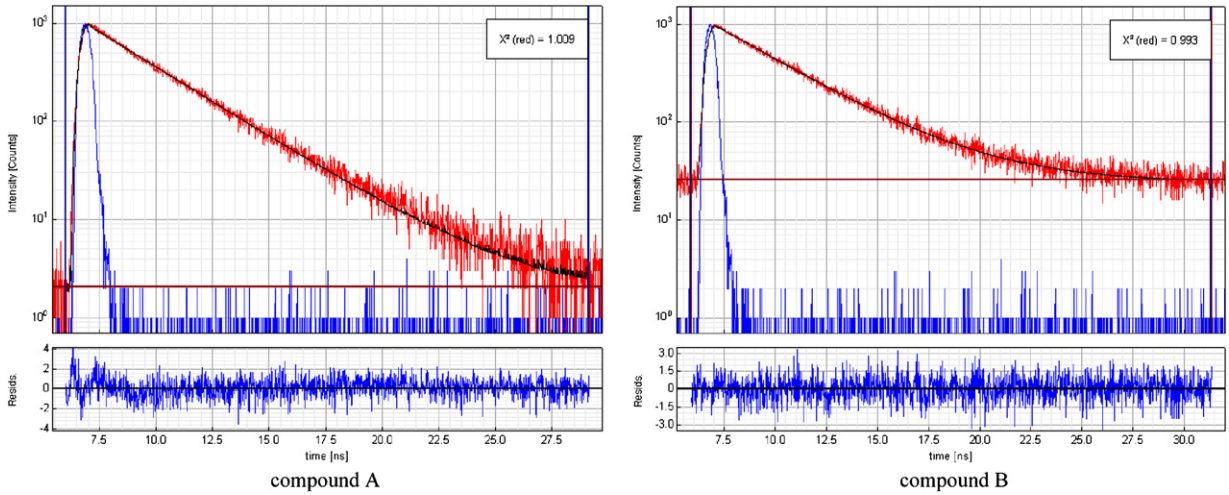

Fig. 6. Typical fluorescence decay profile of the compound A and B in chloroform.

as 136.84°, −137.97°, −97.32° and 99.66° in compound A and B, respectively.

The optimized geometries of the two compounds in the first excited state (S_1) were used as import data to calculate singlet–singlet electronic transition using time-dependent DFT method at the B3LYP/6-31G(d, p) level in different polar solvents, respectively, yielding the vertical electronic transitions energy of $S_1 \rightarrow S_0$. The computed data are collected in Table S3 (in SI). The continuous emission spectra were simulated with the help of SWIZARD software with the width at half-height of 2500 cm^{-1} on the basis of the calculated vertical excited energy and their corresponding oscillator strengths. The simulated emission spectra of two compounds are shown in Fig. S2(in SI). As can be seen in Fig. S2 and Table S3, the electronic transitions are of the $\pi \rightarrow \pi^*$ type. The calculated $S_1 \rightarrow S_0$ emission energy, oscillator strength of the two compounds in different polar solvents are 23,564–23,760 cm^{-1}, 0.5982–0.6448 and 23,416–23,741 cm^{-1}, 0.7133–0.7214, respectively. All the electronic transitions are strongly allowed. The calculated Stoke's shifts of the two compounds are 3936–4042 cm^{-1} and 3810–4227 cm^{-1} in different polar solvents, respectively. The small Stoke's shifts show a consequence of the rigidity of the two compounds. The simulated emission spectra are consist with the experimental fluorescence spectra of two compounds. Simulation emission spectra show the two compounds in different polar solvents can emit blue light and it might be potential luminescent materials with blue light emission.

3.7. Molecular photophysical properties

The fluorescence quantum yields of the compound A and B were measured in different polar solvents at room temperature by a relative method using quinine sulfate in 0.1 M sulphuric acid as a standard solution. The fluorescence quantum yields were calculated from Eq. (6) [45].

$$\Phi_s = \Phi_r \frac{F_s}{F_r} \frac{A_r}{A_s} \left(\frac{n_r}{n_s}\right)^2 \quad (6)$$

where Φ is the fluorescence quantum yield, F is the integration of the emission intensities, n is the index of refraction of the solution, and A is the absorbance at the excitation wavelength, the subscripts "r" and "s" denote the reference and unknown samples, respectively. The fluorescence quantum yields (Φ) are collected in Table 4. As shown in Table 4, these compounds show higher fluorescence quantum yields in different polar solvents.

Table 4
The fluorescence quantum yields (Φ) and the fluorescence lifetimes (τ, ns) of the compound A and B in different polar solvents.

	Solvent	Quantum yield (Φ)	Fluorescence lifetime (τ, ns)
Compound A	Toluene	0.25	2.83
	Ethylacetate	0.30	3.31
	chloroform	0.24	3.04
	DMF	0.29	3.19
	DMSO	0.30	3.24
Compound B	Toluene	0.25	3.55
	Ethylacetate	0.25	3.74
	chloroform	0.10	3.56
	DMF	0.25	3.38
	DMSO	0.22	3.22

The fluorescence decay behaviors of the compound A and B were also studied in different polar solvents. The fluorescence decay curves were recorded with time-correlated single photon counting technique using a commercially available Edinburgh Instruments. Typical decay profiles of the compound A and B are shown in Fig. 6. The fluorescence lifetimes (τ) are also collected in Table 4. For the compound A and B, the fluorescence decay curves are mono-exponential model.

4. Conclusions

In this paper, two novel pyrazoline derivatives 2,8-bis(1,3-diphenyl-pyrazoline-5-yl)dibenzofuran (A) and 2,8-bis(1-(4-bromophenyl)-3-phenyl-pyrazoline-5-yl)dibenzofuran (B) were synthesized and characterized by elemental analysis, NMR, MS and thermogravimetric analysis. The experimental data and conclusions about the structure, UV–vis spectra and fluorescence spectra are supported by quantum chemistry computations. The calculated reorganization energy for hole and electron indicates that the two compounds are in favor of hole transport than electron transport. Our results show that the two novel pyrazoline derivatives exhibit excellent fluorescence quantum yields and high thermal stability, they could be used as excellent optoelectronic materials in organic light-emitting devices. The investigations for their applications are progressing in our laboratory, and the results will be released soon.

Acknowledgements

This work was supported by Shanxi Province scientific and technological project (No. 20100321085) and Fund of Key Laboratory of Optoelectronic Materials Chemistry and Physics, Chinese Academy of Sciences (No. 2011KL004). All the calculations have been performed using the advanced computing facilities of supercomputing center of computer network information center of Chinese Academy of Sciences. All the authors express their deep thanks.

Appendix A. Supplementary data

Supplementary data associated with this article can be found, in the online version, at doi:10.1016/j.saa.2011.08.026.

References

[1] C.W. Tang, S.A. Vanslyke, Appl. Phys. Lett. 51 (1987) 913–915.
[2] J.H. Burroughes, D.D.C. Bradley, A.R. Brown, Nature 347 (1990) 539–541.
[3] Q.X. Tong, S.L. Lai, M.Y. Chan, Chem. Mater. 20 (2008) 6310–6312.
[4] J.N. Moorthy, P. Venkatakrishnan, D.F. Huang, Chem. Commun. 214 (2008) 6–2148.
[5] H.C. Li, Y.P. Lin, P.T. Chou, Y.M. Cheng, R.S. Liu, Adv. Funct. Mater. 17 (2007) 520–530.
[6] C.A. Breen, J.R. Tischler, V. Bulovic, T.M. Swager, Adv. Mater. 17 (2005) 1981–1985.
[7] M. Amir, H. Kumar, S.A. Khan, Bioorg. Med. Chem. Lett. 18 (2008) 918–922.
[8] K. Manna, Y.K. Agrawal, Bioorg. Med. Chem. Lett. 19 (2009) 2688–2692.
[9] M. Abid, A.R. Bhat, F. Athar, A. Azam, Eur. J. Med. Chem. 44 (2009) 417–425.
[10] A. Budakoti, A.R. Bhat, A. Azam, Eur. J. Med. Chem. 44 (2009) 1317–1325.
[11] Z.A. Kaplancikli, G. Turan-Zitouni, A. Özdemir, Ö.D. Can, P. Chevallet, Eur. J. Med. Chem. 44 (2009) 2606–2610.
[12] D. Havrylyuk, B. Zimenkovsky, O. Vasylenko, L. Zaprutko, R. Lesyk, Eur. J. Med. Chem. 44 (2009) 1396–1404.
[13] N. Göhan-Kelekçi, S. Koyunoğlu, S. Yabanoğlu, Bioorg. Med. Chem. 17 (2009) 675–689.
[14] I.G. Rathish, K. Javed, S. Ahmad, S. Bano, Bioorg. Med. Chem. Lett. 19 (2009) 255–258.
[15] F.F. Barsoum, A.S. Girgis, Eur. J. Med. Chem. 44 (2009) 2172–2177.
[16] S.J. Ji, H.B. Shi, Dyes Pigments 70 (2006) 246–250.
[17] J.Y. Pan, U. Scherf, A. Schreiber, R. Bilke, D. Haarer, Synth. Met. 115 (2000) 79–82.
[18] S.R. Sandler, K.C. Tosu, J. Phys. Chem. 39 (1963) 1062–1069.
[19] B.D. Xiao, L. Xi, S.W. Yang, H.B. Fu, Z.G. Shuai, Y. Fang, J.N. Yao, J. Am. Chem. Soc. 125 (2003) 6740–6745.
[20] Y.F. Sun, Y.P. Cui, Dyes Pigments 81 (2009) 27–34.
[21] B. Bian, S.J. Ji, H.B. Shi, Dyes Pigments 76 (2008) 348–352.
[22] X.H. Zhang, W.Y. Lai, S.K. Wu, Chem. Phys. Lett. 320 (2000) 77–80.
[23] X.C. Gao, H. Cao, L.Q. Zhang, B.W. Zhang, Y. Cao, C.H. Huang, J. Mater. Chem. 9 (1999) 1077–1080.
[24] Z.Q. Gao, C.S. Lee, I. Bello, S.T. Lee, S.K. Wu, Z.L. Yan, et al., Synth. Met. 105 (1999) 141–144.
[25] J. Barbera, C. Koen, G. Raquel, H. Stephan, P. Andre, L.S. Jose, J. Mater. Chem. 8 (1998) 1725–1730.
[26] T. Sano, T. Fujii, Y. Nishio, Y. Hamada, K. Shibata, K. Kuroki, Jpn. J. Appl. Phys. Part 1 34 (1995) 3124–3127.
[27] R.H. Young, J.J. Fitzgerald, J. Phys. Chem. 99 (1995) 4230–4240.
[28] P.M. Borsenberger, L.B. Schein, J. Phys. Chem. 98 (1994) 233–239.
[29] M. Jin, Y.J. Liang, R. Lu, X.H. Chuai, Z.H. Yi, Y.Y. Zhao, H.J. Zhang, Synth. Met. 140 (2004) 37–41.
[30] M.L. Wang, J.X. Zhang, J.Z. Liu, C.X. Xu, H.X. Ju, J. Lumin. 99 (2002) 79–83.
[31] G. Bai, J.F. Li, D.X. Li, C. Dong, X.Y. Han, P.H. Lin, Dyes Pigments 75 (2007) 93–98.
[32] Geeta Joshi nee Pant, B.S. Pramod Singh, M.S.M. Rawat, G.C. Rawat, Joshi, Spectrochim. Acta A 78 (2011) 1075–1079.
[33] V. Kanagarajan, M.R. Ezhilarasi, M. Gopalakrishnan, Spectrochim. Acta A 78 (2011) 635–639.
[34] H.-p. Shi, Y. Cheng, W.-j. Jing, J.-B. Chao, L. Fang, X.-Q. Dong, C. Dong, Spectrochim. Acta A 75 (2010) 525–532.
[35] H.-p. Shi, L. Xu, Y. Cheng, J.-y. He, J.-x. Dai, L.-w. Xing, B.-q. Chen, L. Fang, Spectrochim. Acta A 81 (2011) 730–738.
[36] P. Hohenberg, W. Kohn, Phys. Rev. 136 (1964) B864–B871.
[37] W. Kohn, L.J. Sham, Phys. Rev. 140 (1965) A1133–A1138.
[38] J.B. Foresman, M.H. Gordon, J.A. Pople, M.J. Frisch, J. Phys. Chem. 96 (1992) 135–149.
[39] M. Cossi, N. Rega, G. Scalmani, V. Barone, J. Chem. Phys. 114 (2001) 5691–5701.
[40] M. Cossi, G. Scalmani, N. Rega, V. Barone, J. Chem. Phys. 117 (2002) 43–54.
[41] M.J. Frisch, G.W. Trucks, H.B. Schlegel, G.E. Scuseria, M.A. Robb, J.R. Cheeseman, J.A. Montgomery, T. Vreven Jr., K.N. Kudin, J.C. Burant, J.M. Millam, S.S. Iyengar, J. Tomasi, V. Barone, B. Mennucci, M. Cossi, B. Scalmani, G.N. Rega, G.A. Petersson, H. Nakatsuji, M. Hada, M. Ehara, K. Toyota, R. Fukuda, J. Hasegawa, M. Ishida, T. Nakajima, Y. Honda, O. Kitao, H. Nakai, M. Klene, X. Li, J.E. Knox, H.P. Hratchian, J.B. Cross, C. Adamo, J. Jaramillo, R. Gomperts, R.E. Stratmann, O. Yazyev, A.J. Austin, R. Cammi, C. Pomelli, J.W. Ochterski, P.Y. Ayala, K. Morokuma, G.A. Voth, P. Salvador, J.J. Dannenberg, V.G. Zakrzewski, S. Dapprich, A.D. Daniels, M.C. Strain, O. Farkas, D.K. Malick, A.D. Rabuck, K. Raghavachari, J.B. Foresman, J.V. Ortiz, Q. Cui, A.G. Baboul, S. Clifford, J. Cioslowski, B.B. Stefanov, G. Liu, A. Liashenko, P. Piskorz, I. Komaromi, R.L. Martin, D.J. Fox, T. Keith, M.A. Al-Laham, C.Y. Peng, A. Nanayakkara, M. Challacombe, P.M.W. Gill, B. Johnson, W. Chen, M.W. Wong, C. Gonzalez, J.A. Pople, Gaussian 03, Inc., Pittsburgh, PA, 2003.
[42] M. Belletete, J.F. Morin, M. Leclerc, G. Durocher, J. Phys. Chem. A 109 (2005) 6953–6959.
[43] R.A. Marcus, Rev. Mod. Phys. 43 (1993) 599–610.
[44] V. Coropceanu, J. Cornil, D.A. da Silva Filho, Y. Oliver, R. Silbey, J.L. Brédas, Chem. Rev. 107 (2007) 926–952.
[45] J.N. Dmas, G.A. Crobys, J. Phys. Chem. 75 (1971) 991–1024.